THE JOURNAL OF PHYSICAL CHEMISTRY LETTERS
A JOURNAL OF THE AMERICAN CHEMICAL SOCIETY

pubs.acs.org/JPCL

Letter

Azimuth-Resolved Circular Dichroism of Metamaterials

Shuliang Ren, Changji Liu, Kaixuan Xu, Nai Jiang, Fangrong Hu, Ping-Heng Tan, Houzhi Zheng, Xinlong Xu,* Chao Shen,* and Jun Zhang*

Cite This: J. Phys. Chem. Lett. 2022, 13, 1697−1704

Read Online

ACCESS | Metrics & More | Article Recommendations | Supporting Information

ABSTRACT: Chiral optical metamaterials have attracted a great deal of attention due to their intriguing properties with respect to fundamental research and practical applications. For metamaterials with achiral structures, the system composed of metamaterials and obliquely incident light has extrinsic chirality and can produce circular dichroism (CD) effect. However, there have been few studies on the azimuth-dependent CD spectra of achiral metamaterials that have greatly improved our understanding of optical phenomena caused by external chirality. In this work, we experimentally studied the azimuth-dependent CD that originated from the extrinsic chirality of the metamaterials in an asymmetric-U shape and a U-bar-shape gold unit structure, separately. We explain the origin of the CD in the coupling of the macro-electric dipole and magnetic dipole, and the simulation results are in good agreement with the experiment. Our results provide a possible way to build an on-chip azimuth sensor based on azimuth-dependent CD spectra of metamaterials.

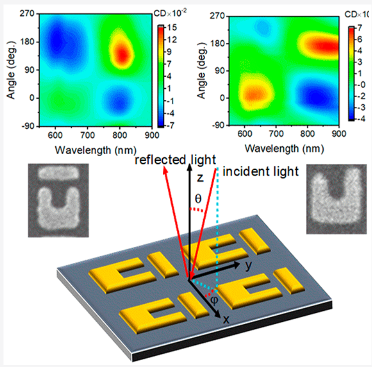

When an object cannot be superposed on its mirror image by rotations or translations, it has chirality. Materials with chirality are omnipresent in nature, from solid crystals to organic macromolecules, such as quartz crystals,[1] perovskites,[2] amino acids,[3] and proteins.[4] Chiral substances are divided into left and right handedness, and they have different responses to left circularly polarized (LCP) light and right circularly polarized (RCP) light.[5,6] Therefore, optical method can be effectively used to study chirality. For example, circular polarization selective Raman spectroscopy can be used to study the vibration characteristics of chiral phonons,[7] circular polarized fluorescence spectroscopy can be used to study the luminescence properties of chiral molecules,[8] and circular dichroism (CD) spectroscopy can directly measure the reflection or transmission difference between LCP and RCP light of the object with a chiral structure or a chiral electronic structure.[9−11] Among the methods mentioned above, CD spectroscopy is widely used to study chirality because of its directness and convenience, and it has very important applications in many fields such analytical chemistry,[12,13] biological monitoring,[10,14] and nano-imaging technology.[15] However, the CD produced by chiral matter in nature is usually very weak, which limits its wide and further application. Because of the development of sample processing technology, metamaterials with chiral structure that responsd in a wide frequency band can be manufactured.[16−18] Metamaterials are kinds of artificial composite structure materials that have properties not present in nature.[19,20] They are usually composed of an array of metallic or dielectric nanostructures.[21] Due to the strong interactions of plasmons in metal nanostructures, they can produce CD that is stronger than that of chiral substances in nature.[22−24] In the past few years, many chiral metamaterials with different geometric structures have been designed to achieve strong CD in broad bands from optical to acoustic wavelengths,[19,25−27] which greatly enriches the fundamental research and practical applications of chiral materials.

In addition to intrinsic chirality in chiral geometric metamaterials, extrinsic chirality can also be induced for the metamaterials with nonchiral planar structures[23,28,29] when the incident light is oblique to the normal direction of the sample. In this case, a system composed of the wave vector of the oblique incident light and the achiral structure does not coincide with its mirror image, so this nonsuperimposable mirror symmetry of the system produces extrinsic chirality.[29,30] Extrinsic chirality has greater tunability, such as changing the angle of the incident light to the normal of the sample, the size of the sample, the symmetry of the unit structure, etc.[23,28,31] At the same time, the extrinsic chirality of the system can be modulated by the azimuth of metamaterials, and the magnitude and sign of CD caused by extrinsic chirality will also change accordingly. Here the azimuth refers to the angle between the direction of the sample symmetry axis and the direction of projection of the incident light on the sample surface. The azimuth-dependent CD spectra have great application prospects for the perception and control of

Received: December 3, 2021
Accepted: February 9, 2022

https://doi.org/10.1021/acs.jpclett.1c03944
J. Phys. Chem. Lett. 2022, 13, 1697−1704

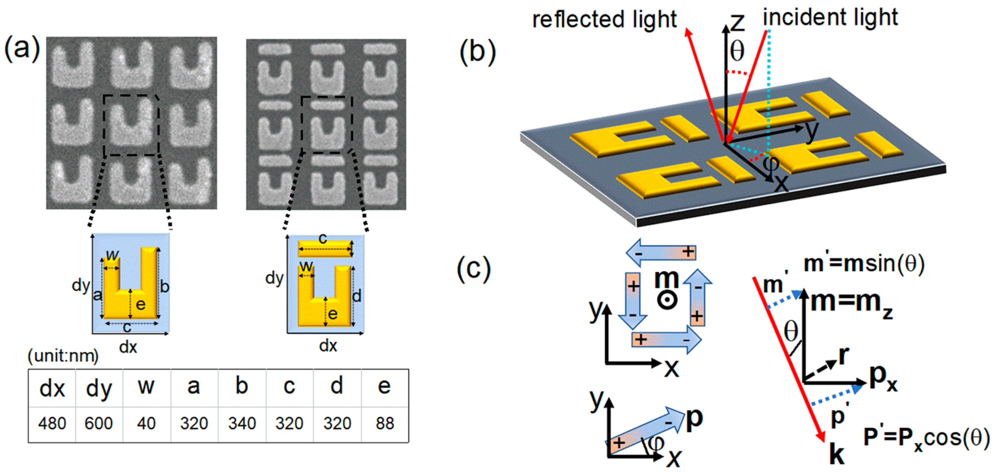

dx	dy	w	a	b	c	d	e
480	600	40	320	340	320	320	88

Figure 1. (a) SEM images of golden metamaterials on an ITO substrate with asymmetric-U shape and U-bar shape unit structures. The geometric parameters are marked in the schematic diagram of the unit structure, and their values are summarized in the table. (b) Experimental configuration for CD measurements, taking the U-bar shape as an example. The x-direction is the bottom of the U-bar shape, and the y-direction is perpendicular to it. The red line represents the incident and reflective circularly polarized light (LCP and RCP) at a certain incident angle θ, and azimuth φ is the angle between the projection of incident light on the sample plane and x-axis. The blue dotted line represents a projection auxiliary line. (c) Schematic diagram in which the dipole current is represented by the arrow and the arrow points in the direction with negative charge. The circular current can induce a magnetic dipole **m**. The total dipole current in any direction is **p**, and the angle between **p** and the x-axis is φ. Their projections along the direction of **r** are **m′** and **p′**, respectively. The black arrow dotted line represents the direction of **r**, and the red arrow line represents the wave vector **k** of incident light.

rotational motion, determination of the azimuth angle of tiny objects as azimuth sensors, detecting the direction of incident light, etc. Although azimuth-dependent CD spectroscopy of three-dimensional (3D) plasmonic metamaterial has been reported,[32] 3D sample processing is more complicated than that of two-dimensional (2D) plasmonic metamaterials. Previous reports of azimuth-dependent CD spectra of 2D plasmonic metamaterials were limited to some special azimuth angles,[29,33] and few experiments have systematically studied the relationship between the azimuth angle and CD in the visible light range.

Here we demonstrate azimuth-dependent optical CD measurements covering the range from −90° to 270° based on the extrinsic chirality of two planar metamaterials, where their unit structures are a planar asymmetric-U shape with weak chirality and a U-bar shape without chirality. We define the bottom of the metamaterial as the x-direction and the direction perpendicular to the bottom as the y-direction. Through theoretical simulation, the dipole current distribution at the characteristic wavelength of CD for metamaterials at an azimuth of 0° is obtained, and the macro-magnetic dipole and electric dipole induced by the dipole current help us to understand the origin of CD from the perspective of the coupling between the magnetic dipole and electric dipole. At the same time, the simulation results of the change in CD with azimuth are in good agreement with the experimental results. The results show that the periodicity of CD changes with azimuth is closely related to the structure of the metamaterial. For asymmetric-U metamaterials, the two characteristic modes of CD originate from the different parts of the structure. At 622 nm, the CD is asymmetric about 90° because the current at the two asymmetric arms plays a major role, while the CD at 840 nm originates from the bottom bar with symmetry about the y-axis; therefore, the CD is the same when the azimuth angles are −90°, 90°, and 270°. For the U-bar shape, the CD at the characteristic wavelength of 660 nm is mainly derived from the two symmetrical arms, so the change in CD with azimuth is symmetrical about the y-axis. Because the widths of the upper and lower bars of the U-bar are not equal, the magnitudes of CD at 800 nm originating from the upper and lower bars before and after 90° of azimuth have obvious differences. Therefore, for a structure that has both symmetrical and asymmetrical elements, from the symmetry of CD with respect to azimuth, we can deduce which part of the structure causes the CD at the characteristic wavelength. For CD modes with symmetry about the azimuth, the azimuth value can be uniquely determined by combining the value of CD and the differential value of d(CD)/d(φ) in the range of −90° to 270°. Due to the convenience of processing metamaterials and the adjustability of external chirality, the development of an azimuth sensor based on such metamaterial is possible.

The metamaterials were fabricated by electron beam lithography (EBL) as described in our previous paper.[34] The material constituting the metamaterial is gold, and its substrate is indium tin oxide (ITO). The scanning electron microscopy (SEM) images, schematic diagram, and geometric parameters of the unit structure are shown in Figure 1a, where we define that the x-direction of the sample is parallel to the bottom bar of the unit structure and the y-direction is perpendicular to the bottom of the unit structure. The unit structures are asymmetric-U and U-bar shapes, respectively. The periods of the unit structures represented by d_x and d_y are 480 and 600 nm, respectively. Their other geometric parameters are summarized in the table in Figure 1a.

■ METHODS

In the CD measurements, supercontinuum white light is dispersed into monochromatic light by an iHR320 monochromator, with a corresponding wavelength range of 550−900 nm. The direction of polarization of the laser and the main axis of the photoelastic modulator (Hinds Instruments, Inc.) present a 45° angle. The photoelastic modulator periodically (50 kHz) modulates the linearly polarized light into LCP and RCP light. Before photoelastic modulation, the incident

https://doi.org/10.1021/acs.jpclett.1c03944
J. Phys. Chem. Lett. 2022, 13, 1697−1704

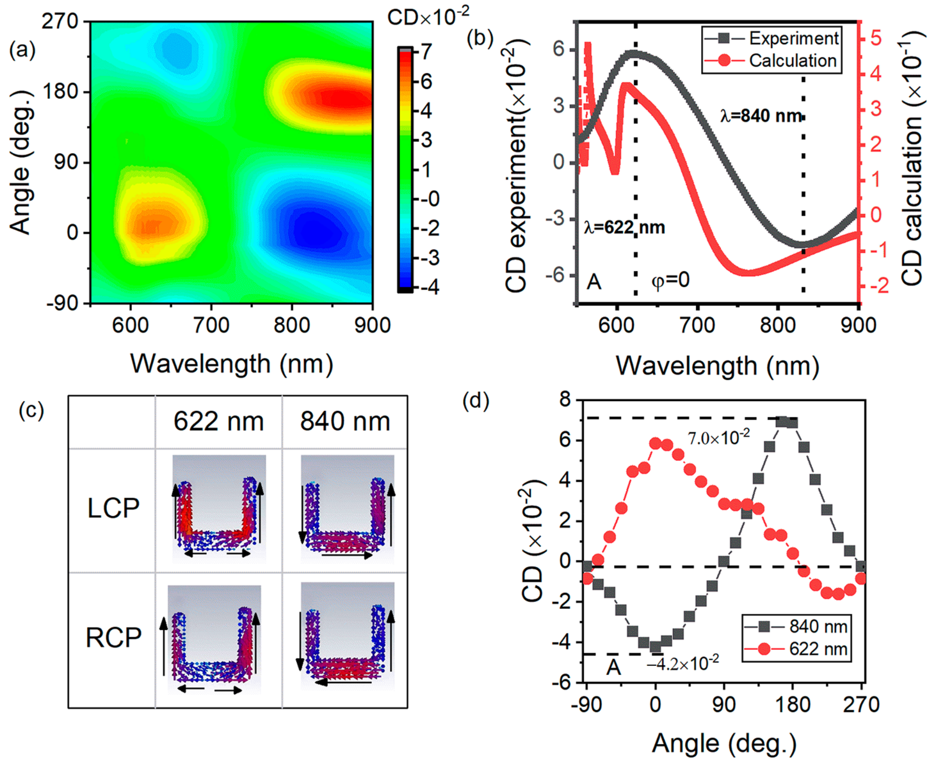

Figure 2. Azimuth-resolved CD spectrum of an asymmetric-U shape. (a) False color mapping of CD spectra of the materials with an asymmetric-U shape. The wavelength is in the range of 550−900 nm, and the azimuth is from −90° to 270°. The red color corresponds to positive CD, and the blue color corresponds to negative CD. (b) Comparison between experimental and simulation results of CD at an azimuth of 0°. Black dotted lines represent experimental results, and the red dotted line represents the simulation result. (c) Macro-dipole current distribution of 622 and 840 nm modes excited by LCP light and RCP light, respectively, in the simulation. Small red arrows correspond to the dipole current induced by high-intensity light. Small blue arrows correspond to the dipole current induced by low-intensity light. Black arrows are macro-current directions based on dipole distributions. (d) Measured azimuth-resolved CD spectra at 622 and 840 nm.

linearly polarized light is modulated by a chopper (SR540) working at 177 Hz. Because the CD signal is weaker than the reflected signal, here we use two lock-in amplifiers (SR830) to obtain the reflection and CD signal simultaneously. The signal synchronized with the chopper corresponds to the sum of the reflected light intensity of LCP and RCP light, while the signal synchronized with the photoelastic modulator is the difference between the reflected light intensity of LCP and RCP light.[35]

In the simulation, electric conductivity σ of gold is set as 4.09×10^7 S m^{-1}. The commercial software (CST Studio) based on a finite element method in the frequency domain solver is employed to simulate the CD spectrum in range of 550−900 nm. The simulated structural parameters are the same with the experimental parameters. The unit cell boundary is set in the x- and y-directions, and the incident port is at an angle of 5° to the z-direction for excitation. The CD spectrum is simulated every 15° of azimuth starting from −90°. The reflection intensity of RCP light is $R_{RCP} = |r_{12}|^2 + |r_{11}|^2$, and the reflection intensity of LCP light is $R_{LCP} = |r_{22}|^2 + |r_{21}|^2$, where r_{ij} represents the reflection coefficient for a reflection with j polarizations at i polarization incidence.

As shown in Figure 1b, the modulated circularly polarized light is incident with a small angle (∼5°) with the normal line on the sample surface; upon deviation from the center of the objective lens, the reflective light can be collected by the same objective lens and detected by the photodiode. Consistent with the general definition, the so-called azimuth is the angle between the projection of the incident light vector on the sample surface and the x-direction of the sample. Taking into account the symmetry of the unit structure, we can change the azimuth in the range of −90° to 270° and measure the value of CD every 15°.

In a medium with a chiral optical response, because the chiral tensor is not zero, the coupling between the electric field vector and the magnetic field vector is a necessary condition for the generation of chiral optical effects.[36] In a system consisting of a metal structure and a dielectric substrate, free electrons in the metal oscillate under light excitation to form plasmons that transmit at the surface and resonate at specific wavelengths. Their motions in a fixed direction can be regarded as a dipole current macroscopically, and the macroscopic circular current can induce a magnetic dipole. The origin of the extrinsic CD effect can be explained from the perspective of the dipole current distribution.[29] As shown in Figure 1c, under incident light excitation, the dipole current generated in the metamaterial plane can be regarded as an electric dipole $\mathbf{p}$, and the circular current in the plane can be equivalent to a magnetic dipole $\mathbf{m}$ perpendicular to the surface of the metamaterial. The magnitude of CD is proportional to the coupling between electric dipoles $\mathbf{p}'$ and magnetic dipoles $\mathbf{m}'$ of metamaterials in the direction perpendicular to the light propagation vector, expressed as CD ∝ $\mathrm{Im}(\mathbf{p}'\cdot\mathbf{m}')$.[37,38] Here, we define $\mathbf{r}$ as the unit vector perpendicular to the propagation direction of incident light, $\mathbf{k}$ as the unit wavevector of the incident light, and θ as the incident angle. The projection components of the electric dipole and magnetic dipole along the $\mathbf{r}$ direction are $\mathbf{m}' = m \sin(\theta)\, \mathbf{r}$ and $\mathbf{p}' = p \cos(\varphi) \cos(\theta)\, \mathbf{r}$, where φ is the azimuth angle. Then we have $\mathbf{p}'\cdot\mathbf{m}' = {}^{1}/_{2}mp$

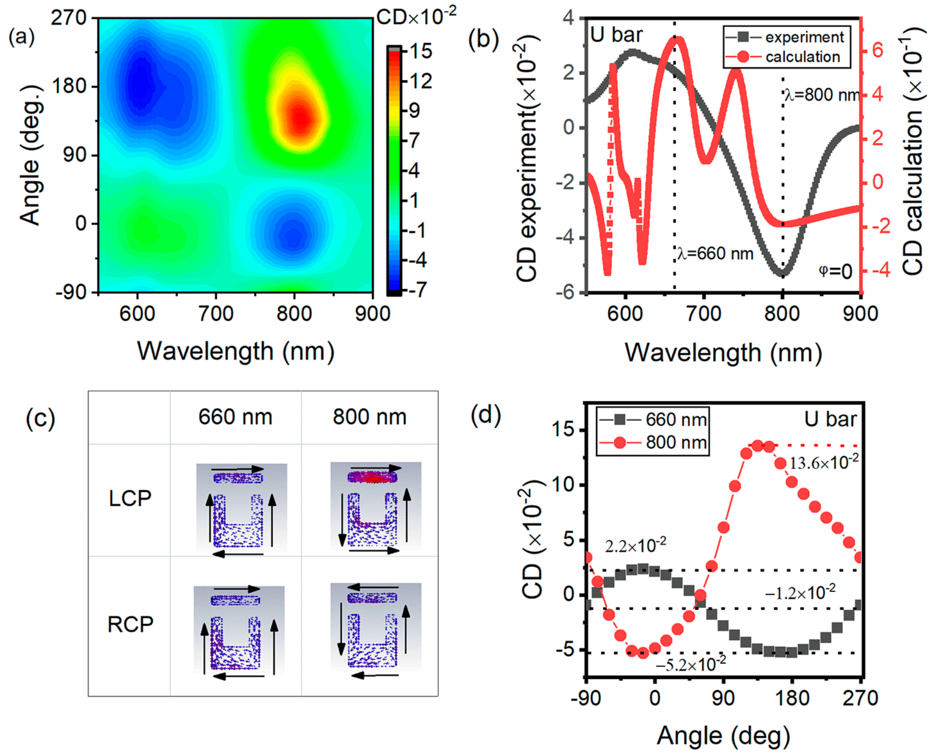

Figure 3. Azimuth-dependent CD spectrum of the U-bar shape. (a) False color mapping of CD spectra of the materials with a U-bar shape. The wavelength is in the range of 550−900 nm, and the azimuth is from −90° to 270°. The red color corresponds to positive CD, and the blue color to negative CD. (b) Comparison between experimental and simulation results of CD at an azimuth of 0°. Black dotted lines represent experimental results, and the red dotted line represents the simulation result. (c) Macro-dipole current distribution of 660 and 800 nm modes excited by LCP light and RCP light, respectively. Small red arrows correspond to the dipole current induced by high-intensity light. Small blue arrows correspond to the dipole current induced by low-intensity light. Black arrows are macro-current directions based on dipole distributions. (d) Measured azimuth-resolved circular dichroism spectra at 660 and 800 nm.

$\cos(\varphi)\sin(2\theta)$. This means that the CD is 0 when the incident light is either perpendicular ($\theta = 0$) or parallel ($\theta = \pi/2$) to the plane of achiral metamaterials.

When incident angle θ is fixed, the CD changes periodically with azimuth φ and the electric dipole plays a major role in the relationship between the CD and azimuth. When azimuth φ is zero, the dipole currents of different unit structures are different, which leads to different CD for different structures. For example, when the dipole current direction is along the y-direction, the angle between the dipole current direction and the x-axis is $\pi/2$, then the electric dipole perpendicular to the light propagation is expressed as $\mathbf{p}' = p\cos(\theta)\cos(\pi/2)$, and the resulting CD signal is close to zero. When the dipole current direction is in the x-direction, the electric dipole perpendicular to the light propagation should be expressed as $\mathbf{p}' = p\cos(\theta)\cos(0)$, and the resulting CD signal approaches the maximum value. Generally, the total electric dipole is the vector sum of the currents in the structure and can be determined according to the simulation and experiment showing which part of the current plays the main role in the CD spectrum.

For the metamaterial with an asymmetric-U shape unit structure. The measured azimuth-dependent CD spectrum is shown in Figure 2a. The azimuth is from −90° to 270°, and wavelength of incident light is in the range of 550−900 nm. The magnitude of CD changes periodically with the azimuth. The maximum value of CD can reach 0.07, and the minimum can reach −0.04. Within the change period of the azimuth, there are two obvious characteristic wavelengths, at 622 and 840 nm. To verify the origins of the CD at the specific wavelength, CST Microwave Studio software was used to simulate the CD spectra, and the simulation results are in good agreement with the experimental results as shown in Figure S1a.

When the azimuth is zero, the simulation result is shown in Figure 2b. In the simulation, the CD signal oscillates in the short wavelength region due to the diffraction behavior with an oblique incidence and a mismatch of the excitation light wavelength and structure period. This is consistent with previous results.[39] The diffraction effect leads to the inability to clearly distinguish CD signals of specific wavelengths. Generally, the diffraction effect is due to the wavelength of the incident light being comparable to the size of the sample. The characteristic size of the unit structure of the asymmetric U-shape metamaterial is ∼600 nm, so the diffraction behavior occurs at short wavelengths in the CD spectrum. Inaccuracy in sample processing may lead to the difference between the CD in the experiment and the simulation results at 840 nm. At the characteristic wavelength of CD of 622 nm, the energy position of the experimental and simulated results is more consistent. Therefore, the simulation can help us understand the origin of CD from the dipole current distribution in the characteristic modes.

As shown in Figure 2c, the simulated current distributions are obtained for the asymmetric-U shape metamaterials under the excitation of LCP light and RCP light. For the mode at 622 nm, under LCP light excitation, the mainly distributed currents in the two arms of the asymmetric-U shape are upward while

https://doi.org/10.1021/acs.jpclett.1c03944
J. Phys. Chem. Lett. 2022, 13, 1697−1704

the current intensity on the left is greater than the current on the right. The current at the bottom diffuses to both sides, and the intensity is smaller than the current at the two arms. The dipole currents formed in the asymmetric-U shape can be regarded as two magnetic dipoles in opposite directions, and the currents in the two arms contribute to the electric dipoles; however, the current at the bottom is still not negligible. Upon excitation by RCP light, the direction of the current distribution is the same as that upon excitation by LCP light, but the current at the right arm is stronger.

For the mode at 840 nm, under LCP light excitation, the current is distributed clockwise on the asymmetric-U shape surface; however, the intensity of the current at the bottom is stronger, so the current can be equivalent to an upward magnetic dipole and a main right electric dipole. Upon excitation by RCP light, the current can be regarded as the coupling of the outward magnetic dipole and the left electric dipole, because the current at the bottom contributes to the main electric dipole.

The relationships between CD and the azimuth at 622 and 840 nm are shown in Figure 2d. When the wavelength is 622 nm, the value of CD is not equal at −90° and 90°, which originates from the current in the two arms asymmetric about the *y*-axis. The intensity of the current in the bottom bar is different; therefore, when the azimuth is 0°, the CD value is not zero. When the wavelength is 840 nm, the CD values are equal at −90° and 90°, which is mainly caused by the current in the bottom bar that is symmetric about the *y*-axis. Therefore, the origin of CD can be determined by observing the symmetry of CD with the azimuth without a specific calculation.

We also studied the azimuth-dependent CD of the U-bar shape metamaterials. Its unit structure is achiral and symmetrical about the *y*-axes. As shown in the Figure 3a, there are two obvious resonant modes in the CD spectrum of the U-bar shape, located at 660 and 800 nm. The maximum CD is 0.15, and the minimum is −0.07. At the same time, for the position of CD and the trend with azimuth, the simulation results are in good agreement with the experimental results as shown in Figure S1b. The magnitude of CD in the simulation is larger than the result of the experiment perhaps due to the loss of the signal in the experiment.

In Figure 3b, we show the experimental and simulation results when the azimuth is 0°. As seen for the asymmetric-U shape, near a wavelength of 660 nm, there is oscillation in the CD simulation, which is possibly due to the diffraction effect, but the position of energy can be considered consistent. In the simulation, there are two characteristic peaks near 660 nm, but in the experiment, it is a continuous broad spectrum that includes the two characteristic peaks. We mainly focus on CD at 660 nm considering the higher intensity and its consistency with other wavelength positions. The characteristic wavelengths of CD at 800 nm in the experimental and simulation result are in good agreement.

In Figure 3c, we show the simulated current distributions of two modes at an azimuth of 0°. When the excitation wavelength is 660 nm, the current excited by the LCP light and the RCP light can be considered as the combination of the counterclockwise circular current and the current upward in the *y*-direction in the right arm of the U-bar. Because the current intensity of RCP light excitation is greater than that of LCP light excitation, this results in a non-zero CD signal at 660 nm.

For the mode at 800 nm, the current excited by the LCP could be considered as a combination of a counterclockwise circular current and a strong rightward current formed at the top bar of the U-bar. The counterclockwise ring current in the U part can be regarded as a magnetic dipole pointing outward to the plane, and the rightward current in the top bar mainly contributes to the electric dipole. The current in the U-bar excited by RCP light can be regarded as a combination of a counterclockwise ring current and a leftward current formed at the bottom bar of the U-bar. The counterclockwise ring current can be regarded as a magnetic dipole pointing outward to the plane, and the leftward current mainly contributes to the electric dipole.

The trends of the variation of CD at 660 and 800 nm with the azimuth are shown in Figure 3d; because the CD at 800 nm is caused by two bars with unequal widths that are symmetrical about the *y*-axis in the U-bar, the values of CD are equal at −90° and 90°, but there is a large difference in intensity between −90° to 90° and 90−270°. While the CD at 660 nm is caused by the two arms at the left and right, they are symmetrical about the *y*-axis and exhibit equal widths. The CD at 660 nm is ~0 when the azimuth is 0° because the current is along the *y*-direction, and the CD reaches the minimum when the azimuth is ~180°. Because the structure of the U-bar is symmetrical about the *y*-axis, but not symmetrical about the *x*-axis, their CD values are not equal at azimuths of 0° and 180°.

The symmetry of the azimuth-dependent CD spectrum at the characteristic wavelength of 800 nm is the same with the structural symmetry, and the minimum CD value deviates significantly from 0. This shows that the main cause of CD is the current in the *x*-direction, which is consistent with the simulation results.

For asymmetric-U and U-bar shapes, the CD that originated from the extrinsic chirality is significantly dependent on the azimuth. Therefore, at the characteristic wavelength, the relationship between the CD and azimuth can be used to make an azimuth sensor, for example, the relationship between the CD and azimuth of the asymmetric-U shape at 840 nm and the relationship between the CD and azimuth of the U-bar shape at 660 nm. The difference in the symmetry of their geometric structure leads to the difference in the symmetry of their azimuth-resolved CD spectrum. For the asymmetric-U shape, it is asymmetric about the *x*- and *y*-directions, but at 840 nm, the CD is mainly from the current at the bottom of the asymmetric-U shape, which is symmetric about the *y*-axis. For the U-bar, it is only symmetric about the *y*-axis, and the value of CD is not equal when the azimuth is −90° and 90°. However, due to the symmetry of the structure, when a CD value is measured, there are two corresponding azimuths, so the azimuth cannot be uniquely determined by only the CD value. However, their changing trend with azimuth is opposite at different azimuth regimes even for the same values of CD, so the azimuth can be uniquely determined by checking the differential curve of the azimuth-dependent CD spectrum.

In Figure 4a, we plot the first-order differential spectrum of the angle-resolved experimental CD spectrum at 840 nm of the asymmetric-U shape and at 660 nm of the U-bar shape metamaterials. The value of the first-order differential spectrum has opposite signs on the two sides of the specific degree of azimuth, which ensures that the value of the azimuth can be identified by combining the CD value and the value of the first-order differential spectrum $\delta = \mathrm{d(CD)}/\mathrm{d}(\varphi)$ of the CD spectrum.

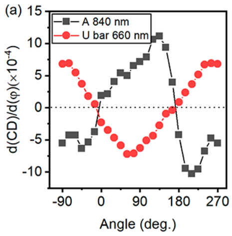

(b)

U bar 660 nm	d(CD)/d(φ) positive	d(CD)/d(φ) negative
CD (-0.012—0.022)	-90-0°	0-90°
CD (-0.052— -0.012)	180-270°	90-180°

A 840 nm	d(CD)/d(φ) positive	d(CD)/d(φ) negative
CD (-0.042—0)	0-90°	-90-0°
CD (0—0.070)	90-180°	180-270°

Figure 4. (a) Azimuth-dependent first-order differential CD spectrum $d(CD)/d(\varphi)$ at 800 nm of the asymmetric-U shape and at 660 nm of the U-bar shape. (b) For the asymmetric-U (A) and U-bar shapes, due to the symmetry of the structure, the range of the CD values and the sign of $d(CD)/d(\varphi)$ jointly can uniquely determine the azimuth.

In Figure 4b, we summarize the azimuth range determined by the range of CD values and the sign of δ at the specific wavelength for the asymmetric-U shape and U-bar shape, respectively. For the asymmetric-U shape at 840 nm, when the CD is in the range of −0.042 to 0.07 and the δ is positive, the detectable azimuth is 0−90°; when the δ is negative, the detectable azimuth is in the range of −90° to 0°. When the CD is from 0 to 0.07 and the δ is positive, the detectable azimuth is in the range of 90−180°; when the δ is negative, the detectable azimuth is in the range of 180−270°. For the U-bar shape, when the CD is in the range of −0.012 to 0.022 and the δ is positive, the detectable azimuth is in the range of −90° to 0°, and when the δ is negative, the detectable azimuth is in the range of 0−90°. When the CD is in the range of −0.052 to −0.012 and the δ is positive, the detectable azimuth is in the range of 180−270°, and when the δ is negative, the detectable azimuth is in the range of 90−180°. The CDs of the two shapes of metamaterials have different dependences on the azimuth, but all of their azimuth sensitivity can reach 10^{-4} deg^{-1}. In the experiment, our system precision of CD is on the order of 10^{-5}. This means we can detect azimuthal changes of >1° using azimuth-resolved CD spectrum.

In summary, we experimentally studied azimuth-dependent CD spectra that are caused by the extrinsic chirality of gold metamaterials with asymmetric-U and U-bar shape basic units in the optical band through oblique incidence. The small incident/reflective angle (∼5°) achieved by striking the incident light on the edge of the same one objective lens ensures the high spatial resolution and stable measurements over the whole range of −90° to 270°. With the help of the simulation results, we can obtain the dipole current distribution and identify the resonant modes in CD spectra. The dipole current can induce macro-electric dipoles and magnetic dipoles, and their interaction with the light field constitutes the physical origin of the CD effect. The asymmetric-U shape and U-bar shape have different symmetries, and the periodicity of the changes in CD with the azimuth is closely related to the structure of the metamaterial. In our experiment, the azimuth-resolved CD signal is highly sensitive, reaching a value of 10^{-4} deg^{-1}. Considering the experimental accuracy, an azimuth sensitivity of better than 1° can be distinguished. Therefore, the azimuth sensor can be made by using the relationship between the CD and azimuth. Due to the existence of symmetry of the asymmetric-U and U-bar shapes, when a CD value is measured, there are usually two azimuths corresponding to it in the whole period (−90° to 270°), but the azimuth value can be uniquely determined by combining the value of the CD spectrum and the value of the first-order differential spectrum $d(CD)/d(\varphi)$. Our results provide an effective solution for on-chip azimuth sensors based on the azimuth-resolved circular dichroism of metamaterials.

■ ASSOCIATED CONTENT

Supporting Information

The Supporting Information is available free of charge at https://pubs.acs.org/doi/10.1021/acs.jpclett.1c03944.

Simulation results of the CD from 550 to 900 nm of metamaterials with asymmetri-U and U-bar shape unit structures as a function of the azimuth from −90° to 270° (PDF)

■ AUTHOR INFORMATION

Corresponding Authors

Jun Zhang − *State Key Laboratory of Superlattices and Microstructures, Institute of Semiconductors, Chinese Academy of Sciences, Beijing 100083, China; Center of Materials Sciences and Optoelectronics Engineering, University of Chinese Academy of Sciences, Beijing 100049, China; CAS Center of Excellence in Topological Quantum Computation, University of Chinese Academy of Sciences, Beijing 101408, China; Beijing Academy of Quantum Information Sciences, Beijing 100193, China;* orcid.org/0000-0002-9831-6796; Email: zhangjwill@semi.ac.cn

Chao Shen − *State Key Laboratory of Superlattices and Microstructures, Institute of Semiconductors, Chinese Academy of Sciences, Beijing 100083, China; Center of Materials Sciences and Optoelectronics Engineering, University of Chinese Academy of Sciences, Beijing 100049, China;* orcid.org/0000-0002-3664-4874; Email: shenchao@semi.ac.cn

Xinlong Xu − *Shaanxi Joint Lab of Graphene, State Key Lab Incubation Base of Photoelectric Technology and Functional Materials, International Collaborative Center on Photoelectric Technology and Nano Functional Materials, Institute of Photonics & Photon-Technology, Northwest University, Xi'an 710069, China;* orcid.org/0000-0002-3034-810X; Email: xlxuphy@nwu.edu.cn

Authors

Shuliang Ren − *State Key Laboratory of Superlattices and Microstructures, Institute of Semiconductors, Chinese Academy of Sciences, Beijing 100083, China; Center of Materials Sciences and Optoelectronics Engineering, University of Chinese Academy of Sciences, Beijing 100049, China;* orcid.org/0000-0001-7708-9398

Changji Liu − *Shaanxi Joint Lab of Graphene, State Key Lab Incubation Base of Photoelectric Technology and Functional Materials, International Collaborative Center on Photoelectric Technology and Nano Functional Materials, Institute of Photonics & Photon-Technology, Northwest University, Xi'an 710069, China*

Kaixuan Xu − *State Key Laboratory of Superlattices and Microstructures, Institute of Semiconductors, Chinese Academy of Sciences, Beijing 100083, China; Center of Materials Sciences and Optoelectronics Engineering, University of Chinese Academy of Sciences, Beijing 100049, China*

Nai Jiang − *State Key Laboratory of Superlattices and Microstructures, Institute of Semiconductors, Chinese Academy of Sciences, Beijing 100083, China; Center of*

https://doi.org/10.1021/acs.jpclett.1c03944
J. Phys. Chem. Lett. 2022, 13, 1697−1704

Materials Sciences and Optoelectronics Engineering, University of Chinese Academy of Sciences, Beijing 100049, China

Fangrong Hu − *Guangxi Colleges and Universities Key Laboratory of Optoelectronic Information Processing, Guilin University of Electronic Technology, Guilin 541004, China;* orcid.org/0000-0003-2835-1980

Ping-Heng Tan − *State Key Laboratory of Superlattices and Microstructures, Institute of Semiconductors, Chinese Academy of Sciences, Beijing 100083, China; Center of Materials Sciences and Optoelectronics Engineering, University of Chinese Academy of Sciences, Beijing 100049, China;* orcid.org/0000-0001-6575-1516

Houzhi Zheng − *State Key Laboratory of Superlattices and Microstructures, Institute of Semiconductors, Chinese Academy of Sciences, Beijing 100083, China; Center of Materials Sciences and Optoelectronics Engineering, University of Chinese Academy of Sciences, Beijing 100049, China*

Complete contact information is available at:
https://pubs.acs.org/10.1021/acs.jpclett.1c03944

Notes

The authors declare no competing financial interest.

■ ACKNOWLEDGMENTS

J.Z. acknowledges support from the National Key R&D Program of China (2017YFA0303401), the CAS Interdisciplinary Innovation Team, and the Strategic Priority Research Program of Chinese Academy of Sciences (XDB28000000). C.S. acknowledges the support from the Youth Innovation Promotion Association, Chinese Academy of Sciences (2019114), and the Strategic Priority Research Program of Chinese Academy of Sciences (XDB30000000).

■ REFERENCES

(1) Winkelmann, A.; Nolze, G. Chirality Determination of Quartz Crystals Using Electron Backscatter Diffraction. *Ultramicroscopy* **2015**, *149*, 58−63.

(2) Ma, J.; Fang, C.; Chen, C.; Jin, L.; Wang, J.; Wang, S.; Tang, J.; Li, D. Chiral 2d Perovskites with a High Degree of Circularly Polarized Photoluminescence. *ACS Nano* **2019**, *13*, 3659−3665.

(3) Liu, X.; Dong, S.; Lin, L.; Feng, X. Chiral Amino Acids-Derived Catalysts and Ligands. *Chin. J. Chem.* **2018**, *36*, 791−797.

(4) Efimov, A. V. Chirality and Handedness of Protein Structures. *Biochemistry (Moscow)* **2018**, *83*, S103−S110.

(5) Chen, C.; Gao, L.; Gao, W.; Ge, C.; Du, X.; Li, Z.; Yang, Y.; Niu, G.; Tang, J. Circularly Polarized Light Detection Using Chiral Hybrid Perovskite. *Nat. Commun.* **2019**, *10*, 1927.

(6) Zhou, J.; Chowdhury, D. R.; Zhao, R.; Azad, A. K.; Chen, H.-T.; Soukoulis, C. M.; Taylor, A. J.; O'Hara, J. F. Terahertz Chiral Metamaterials with Giant and Dynamically Tunable Optical Activity. *Phys. Rev. B* **2012**, *86*, 035448.

(7) Xu, B.; Mao, N.; Zhao, Y.; Tong, L.; Zhang, J. Polarized Raman Spectroscopy for Determining Crystallographic Orientation of Low-Dimensional Materials. *J. Phys. Chem. Lett.* **2021**, *12*, 7442−7452.

(8) Anetai, H.; Takeda, T.; Hoshino, N.; Araki, Y.; Wada, T.; Yamamoto, S.; Mitsuishi, M.; Tsuchida, H.; Ogoshi, T.; Akutagawa, T. Circular Polarized Luminescence of Hydrogen-Bonded Molecular Assemblies of Chiral Pyrene Derivatives. *J. Phys. Chem. C* **2018**, *122*, 6323−6331.

(9) Zhou, Y.; Sethi, G.; Zhang, C.; Ni, X.; Liu, F. Giant Intrinsic Circular Dichroism of Enantiomorphic Flat Chern Bands and Flatband Devices. *Phys.Rev. B* **2020**, *102*, 125115.

(10) Miles, A. J.; Janes, R. W.; Wallace, B. A. Tools and Methods for Circular Dichroism Spectroscopy of Proteins: A Tutorial Review. *Chem. Soc. Rev.* **2021**, *50*, 8400−8413.

(11) Ahn, J.; Ma, S.; Kim, J. Y.; Kyhm, J.; Yang, W.; Lim, J. A.; Kotov, N. A.; Moon, J. Chiral 2d Organic Inorganic Hybrid Perovskite with Circular Dichroism Tunable over Wide Wavelength Range. *J. Am. Chem. Soc.* **2020**, *142*, 4206−4212.

(12) Koenis, M. A. J.; Tiekink, E. H.; Van Raamsdonk, D. M. E.; Joosten, N. U.; Gooijer, S. A.; Nicu, V. P.; Visscher, L.; Buma, W. J. Analytical Chemistry on Many-Center Chiral Compounds Based on Vibrational Circular Dichroism: Absolute Configuration Assignments and Determination of Contaminant Levels. *Anal. Chim. Acta* **2019**, *1090*, 100−105.

(13) Kurouski, D. Advances of Vibrational Circular Dichroism (Vcd) in Bioanalytical Chemistry. A Review. *Anal. Chim. Acta* **2017**, *990*, 54−66.

(14) Zhang, H.; et al. In Situ Monitoring of Molecular Aggregation Using Circular Dichroism. *Nat. Commun.* **2018**, *9*, 4961.

(15) Tudahong, A.; Qu, Y.; Bai, J.-R.; Zhang, Z.-Y. Studies of Circular Dichroism of Planar Composite Metal Nanostructure Arrays. *Acta Physica Sinica* **2020**, *69*, 107802.

(16) Lu, M. H.; Feng, L.; Chen, Y. F. Phononic Crystals and Acoustic Metamaterials. *Mater. Today* **2009**, *12*, 34−42.

(17) Kumar, P.; Ali, T.; Pai, M. M. M. Electromagnetic Metamaterials: A New Paradigm of Antenna Design. *IEEE Access* **2021**, *9*, 18722−18751.

(18) Vynck, K.; Felbacq, D.; Centeno, E.; Cabuz, A. I.; Cassagne, D.; Guizal, B. All-Dielectric Rod-Type Metamaterials at Optical Frequencies. *Phys. Rev. Lett.* **2009**, *102*, 133901.

(19) Oh, S. S.; Hess, O. Chiral Metamaterials: Enhancement and Control of Optical Activity and Circular Dichroism. *Nano Convergence* **2015**, *2*, 24.

(20) Zhu, S.; Zhang, X. Metamaterials: Artificial Materials Beyond Nature. *National Science Review* **2018**, *5*, 131−131.

(21) Zheludev, N. I. The Road Ahead for Metamaterials. *Science* **2010**, *328*, 582−583.

(22) Fan, Z.; Govorov, A. O. Plasmonic Circular Dichroism of Chiral Metal Nanoparticle Assemblies. *Nano Lett.* **2010**, *10*, 2580−7.

(23) Cao, T.; Wei, C.; Mao, L.; Li, Y. Extrinsic 2d Chirality: Giant Circular Conversion Dichroism from a Metal-Dielectric-Metal Square Array. *Sci. Rep.* **2015**, *4*, 7442.

(24) Cao, T.; Cryan, M. J. Enhancement of Circular Dichroism by a Planar Non-Chiral Magnetic Metamaterial. *J. Opt.* **2012**, *14*, 085101.

(25) Wang, C.; Li, Z.; Pan, R.; Liu, W.; Cheng, H.; Li, J.; Zhou, W.; Tian, J.; Chen, S. Giant Intrinsic Chirality in Curled Metasurfaces. *ACS Photonics* **2020**, *7*, 3415−3422.

(26) Zhu, A. Y.; Chen, W. T.; Zaidi, A.; Huang, Y. W.; Khorasaninejad, M.; Sanjeev, V.; Qiu, C. W.; Capasso, F. Giant Intrinsic Chiro-Optical Activity in Planar Dielectric Nanostructures. *Light Sci. Appl.* **2018**, *7*, 17158.

(27) Lee, Y. Y.; Kim, R. M.; Im, S. W.; Balamurugan, M.; Nam, K. T. Plasmonic Metamaterials for Chiral Sensing Applications. *Nanoscale* **2020**, *12*, 58−66.

(28) Fan, J.; Xiao, D.; Lei, T.; Yuan, X. Incidence Angle-Dependent Broadband Chiral Metamaterial for near-Infrared Light Absorption. *Journal of the Optical Society of America B* **2020**, *37*, 3422−3428.

(29) Zhang, Y.; Wang, L.; Zhang, Z. Circular Dichroism in Planar Achiral Plasmonic L-Shaped Nanostructure Arrays. *IEEE Photonics Journal* **2017**, *9*, 1−7.

(30) Pellegrini, G.; Finazzi, M.; Celebrano, M.; Duò, L.; Biagioni, P. Chiral Surface Waves for Enhanced Circular Dichroism. *Phys. Rev. B* **2017**, *95*, 241402.

(31) Plum, E.; Fedotov, V. A.; Zheludev, N. I. Extrinsic Electromagnetic Chirality in Metamaterials. *Journal of Optics A: Pure and Applied Optics* **2009**, *11*, 074009.

(32) Hou, Y.; Leung, H. M.; Chan, C. T.; Du, J.; Chan, H. L.-W.; Lei, D. Y. Ultrabroadband Optical Superchirality in a 3d Stacked-Patch Plasmonic Metamaterial Designed by Two-Step Glancing Angle Deposition. *Adv. Funct. Mater.* **2016**, *26*, 7807−7816.

(33) Maoz, B. M.; Ben Moshe, A.; Vestler, D.; Bar-Elli, O.; Markovich, G. Chiroptical Effects in Planar Achiral Plasmonic Oriented Nanohole Arrays. *Nano Lett.* **2012**, *12*, 2357−2361.
(34) Zhang, J.; Cao, C.; Xu, X.; Liow, C.; Li, S.; Tan, P. H.; Xiong, Q. Tailoring Alphabetical Metamaterials in Optical Frequency: Plasmonic Coupling, Dispersion, and Sensing. *ACS Nano* **2014**, *8*, 3796−3806.
(35) Wu, Y. J.; Shen, C.; Tan, Q. H.; Shi, J.; Liu, X. F.; Wu, Z. H.; Zhang, J.; Tan, P. H.; Zheng, H. Z. Valley Zeeman Splitting of Monolayer Mos2 Probed by Low-Field Magnetic Circular Dichroism Spectroscopy at Room Temperature. *Appl. Phys. Lett.* **2018**, *112*, 153105.
(36) Qiu, M.; Zhang, L.; Tang, Z.; Jin, W.; Qiu, C.-W.; Lei, D. Y. 3D Metaphotonic Nanostructures with Intrinsic Chirality. *Adv. Funct. Mater.* **2018**, *28*, 1803147.
(37) Sihvola, A. H.; Viitanen, A. J.; Lindell, I. V.; Tretyakov, S. A. *Electromagnetic Waves in Chiral and Bi-Isotropic Media*; Artech House: London, 1994.
(38) Liu, N.; Giessen, H. Coupling Effects in Optical Metamaterials. *Angew. Chem., Int. Ed. Engl.* **2010**, *49*, 9838−52.
(39) Feng, C.; Wang, Z. B.; Lee, S.; Jiao, J.; Li, L. Giant Circular Dichroism in Extrinsic Chiral Metamaterials Excited by Off-Normal Incident Laser Beams. *Opt. Commun.* **2012**, *285*, 2750−2754.

https://doi.org/10.1021/acs.jpclett.1c03944
J. Phys. Chem. Lett. 2022, 13, 1697−1704